Acta Scientific Pharmaceutical Sciences

Volume 1 Issue 5 November 2017

Research Article

3D-QSAR and Pharmacophore Identification Studies Applied to Pyridazin-3-one Derivatives as Potent PDE4 Inhibitors

Edeildo F da Silva-Júnior[1,2]*, Thiago M de Aquino[2] and João X de Araújo-Júnior[1,2]

[1]*Laboratory of Medicinal Chemistry, Nursing and Pharmacy School, Federal University of Alagoas, Lourival Melo Motta Avenue, Tabuleiro dos Martins, Maceió, Brazil*

[2]*Chemistry and Biotechnology Institute, Federal University of Alagoas, Lourival Melo Motta Avenue, Tabuleiro dos Martins, Maceió, Brazil*

***Corresponding Author:** Edeildo F da Silva-Júnior, Laboratory of Medicinal Chemistry, Federal University of Alagoas, Maceió, Alagoas, Brazil.

Received: September 13, 2017; **Published:** October 27, 2017

Abstract

Phosphodiesterase-4 (PDE4) is the most predominant subtype of PDEs present in cells. This enzyme is responsible for cAMP-specific inactivation to 5'-AMP via hydrolysis and it has been associated with several inflammatory disorders. The aim of this study was to find molecular features from the pyridazin-3-one class in tentative to elucidate a 3D-Quantitative Structure-Activity Relationship (3D-QSAR) to provide useful information for the design of new compounds. In the present work, we report the (3D-QSAR), Partial Least-Square (PLS) with Leave-One-Out (LOO) as cross-validation method and pharmacophore identification studies. The satisfactory statistical validation (r^2 = 0.97 and 0.98, q^2 = 0.95 and 0.97, F-test = 89.46 and 341.07, pred_r^2 = 0.83 and 0.85) from two mathematical models built was obtained by Multiple Linear Regression (MLR) and Stepwise (SW) methods. In addition, pharmacophore model study revealed the importance of some features (two hydrogen bond acceptor, one hydrogen bond donor, and one aromatic ring). Finally, the correlation analysis between all results provides a solid basis for the future rational design of more active and more selective PDE4 inhibitors.

Keywords: PDE4; Pyridazin-3-one; 3D-QSAR; Pharmacophore Model

Introduction

The subclass of phosphodiesterase (PDE) comprises an attractive target for the design of new therapeutic agents [1]. The PDE enzyme catalysis the specific hydrolysis of the cyclic adenosine 3',5'-monophosphate (cAMP) and cyclic guanosine 3',5'-monophosphate (cGMP) into their corresponding 3',5'-nucleotide (AMP and GMP) in cells [2-5]. cAMP and cGMP are intracellular second messengers able to mediate the response of cells to a variety of hormones and neurotransmitters in signal transduction pathways [6]. The levels of these second messengers can be controlled by alterations in the PDE activities [3].

PDE4 is among the eleven known phosphodiesterase isoforms (PDE1-11) and it is the most predominant subtype present on cells [3,7-9]. This cyclic nucleotide is responsible by cAMP-specific inactivation, via hydrolysis to 5'-AMP [10,11]. Moreover, it is mainly found in airway smooth muscle, immune and inflammatory cells, and in the brain [3]. PDE4 is associated with several inflammatory disorders, such as asthma, chronic obstructive pulmonary disease (COPD), schizophrenia, stroke, osteoporosis and rheumatoid arthritis [3,5,7,8]. In this sense, cAMP-specific PDE4 is believed to play a central role in inflammatory processes [12]. Many classes of compounds and drugs are reported as PDE4 inhibitors, including Rolipram and their analogs RP73401, Zardaverine, as well, Cilomilast, *rac*-CMPI, and *rac*-CMPO [13].

Cheminformatics techniques are broadly employed for the analysis of active compounds, resulting in models applied to design novel active molecules or virtual screening of databases using the model as a query [14]. Quantitative Structure-Activity Relationship (QSAR) describe the dependence of the biological activity of the chemical structures based on a set of active molecules [15]. In general, the QSAR approach became an important tool for automated pre-virtual screening, combinatorial library design, and data mining [5]. In addition, this approach is routinely used in modern drug design to aid the understanding of drug-receptor interactions, based on pharmacophore model [9,16,17]. The 3D-QSAR technique represents the most successful and broadly used ligand-based drug design (LBDD) approach for estimating activity within a specific chemical series of ligands and for guiding the synthesis of novel analogs [18]. The application of hydrophobic, steric and electrostatic fields comprise an interesting pathway to improve quality and predictivity to the 3D-QSAR models [18].

Previously, our research group reported studies involving the inhibitory activity of 6-aryl pyridazin-3-one analogs. Results revealed that some compounds present similar potency that Rolipram, an approved drug [1,19]. Now, we attempted to elucidate a structure-activity relationship to provide useful information for the design and synthesis of more potent pyridazin-3-ones and related compounds with predetermined activities. In order to goal the aims, we report the building of 3D-QSAR models, cross-validated by Partial Least Squares (PLS) with Leave-One-Out (PLS-LOO) method and pharmacophore identification applied to the set of PDE4 inhibitors previously synthesized.

Materials and Methods

Compounds library

Initially, a dataset of 30 pyridazin-3-one compounds was drawn using Marvin Sketch [20]. The 2D-structures were converted into 3D using VLife MDS version 4.6 program [20-22]. The dataset was divided into a training set (80%, 24 molecules) and test set (20%, 6 molecules) on the basis of chemical and biological diversity using Sphere Exclusion method (Table 1) [21,22]. For compounds with determined IC_{50}, the pIC_{50} values were obtained using -log (IC_{50}). With regard to compounds with no IC_{50} values (only showing the percentage of inhibition), -log (% inhibition) was used as a parameter.

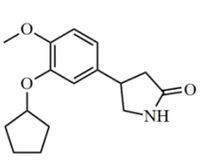

Rolipram

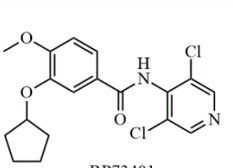

RP73401

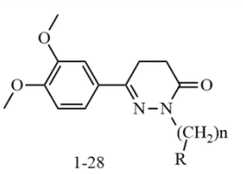

1-28

Code	n	R	Dataset	pIC_{50}
1	0	H	Test	5.69
2	0	Phenyl	Training	6.25
3	1	Phenyl	Test	7.22
4	3	Phenyl	Training	7.69
5	3	OH	Training	1.89[c]
6	6	OH	Training	6.6
7	3	$CO_2CH_2CH_3$	Training	6.56
8	4	CO_2CH_3	Test	6.76
9	1	COOH	Test	1.41[c]
10	3	COOH	Training	1.84[c]
11	4	COOH	Training	5.85
12	4	CONHOH	Training	5.48
13	1	$CONH_2$	Training	1.76[c]
14	1	DMB[a]	Training	6.11
15	3	DMB[a]	Training	6.22
16	1	Thiomorpholinecarbamide	Training	1.94[c]
17	3	Thiomorpholinecarbamide	Training	1.93[c]
18	3	4-Methyl-thiomorpholinecarbamide	Training	1.92[c]
19	3	NHBOC[b]	Training	6.31
20	6	NHBOC[b]	Training	7.22
21	6	NHCOPh	Training	7.52
22	6	DMB[a]	Training	1.93[c]
23	6	Piperidine	Training	1.2[c]
24	6	NH_2	Training	7.69
25	6	Morpholine	Training	6.74
26	6	Thiomorpholine	Training	6.67
27	6	4-Methyl-piperazine	Test	6.4
28	0	Cyclopentyl	Training	6.2
Rolipram	-	-	Test	6.22
RP73401	-	-	Training	9.0

Table 1: Molecules used to build 3D-QSAR models.

a: 2,4-dimethoxybenzyl; b: tert-butyloxycarbonyl; c: values calculated using log (% inhibition).

3D-Quantitative Structure-Activity (3D-QSAR) Analysis

Molecular Alignment

6-Phenyl-4,5-dihydropyridazin-3-one structure was used as a template to build the dataset by using VLife MDS version 4.6, with an RMSD value ≤ 0.1 Å [23,24]. Initially, the molecular geometries were optimized through the Merck Molecular Force Field (MMFF) [2,8,24]. Charges were assumed as Gasteiger-Marsili type [24]. The molecular alignment of all pyridazines from the dataset is shown in figure 1.

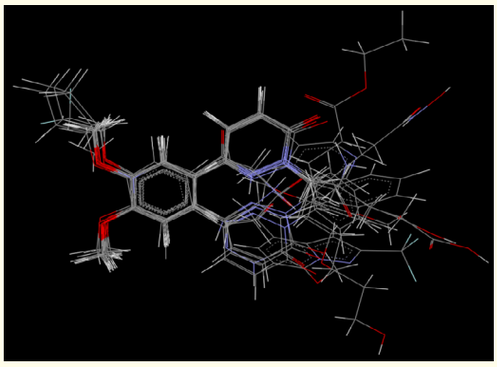

Figure 1: Molecular alignment for pyridazin-3-one derivatives in this study.

3D-Descriptors

All 3D molecular descriptors were generated using VLife MDS version 4.6 [23,24]. This step was followed by the rectangular grid generation surrounding all molecules in the dataset and a column containing in pIC_{50} was added. Hydrophobic, steric and electrostatic fields were computed (total = 8317 3D-descriptors) at the lattice points of the grid using a methyl probe of charge +1 [2,24]. Additionally, all the invariable columns were excluded. The activities were assumed as dependent variables whereas all 3D-descriptors were presumed as independent variables. Furthermore, several search algorithms were investigated, such as stepwise (SW) forward-backward variable selection method, genetic algorithm (GA), simulated annealing (SA), and multiple linear regression (MLR). These methods are the most commonly used for building QSAR models and can explain different situations (active and inactive compounds) [21]. Finally, the radar plot graphics were generated using VLife MDS version 4.6 in order to evaluate the prediction in training and test groups by the 3D-QSAR equations.

3D-QSAR model validation

The relationship between dependent and independent variables (activities and 3D-computed fields, respectively) were obtained by regression analysis [24]. The quality of the quantitative models generated was provided by statistical parameters application, such as r^2, q^2, F-test, variance cut-off as 0.1 and number of random interactions as 100 [20,23]. Models with q^2 values less than 0.7 were discarded [20]. In accordance with Golbraikh., *et al.* [25] a quantitative model is considered to be robust when it fulfills the conditions: $r^2 > 0.6$, $q^2 > 0.6$ and pred_$r^2 > 0.5$. Finally, high F-test values suggest that the model is statistically significant [20]. The validation for the 3D-QSAR equations is a very important aspect in the drug design studies [23]. In 3D-QSAR, usually Partial Least Squared (PLS) is performed to correlate the molecular structures of ligands to their biological activity [18]. In an attempt to get a better insight into the molecular descriptor space, the PLS analysis was performed [17]. The most common method to evaluate the robustness is the analysis of the influence of each descriptor over a final equation [23]. Normally, that process is performed by cross-validation, including Leave-One-Out (LOO) method which is broadly employed in 3D-QSAR validations [8,20,23]. After the 3D-QSAR building, the PLS analysis was performed using the selected descriptors from the mathematical models, and the cross-validation was performed.

Pharmacophore model

The development of the pharmacophore model was performed using VLife MDS version 4.6 [2,24]. In general, the pharmacophore model is a 3D-representation of features which should be present in active ligands [2,24]. Initially, the PDE4-inhibitors dataset was aligned with the most active molecule [24]. In the final model, the maximum number of admitted features was five, with a distance lower than 10 Å between them [24]. The Root Mean-Squared Deviation (RMSD) average for each peer of the aligned molecule was established as 0.05 Å [2].

Results and Discussion

3D-Quantitative Structure-Activity Relationship (3D-QSAR) analysis

The 3D-QSAR analysis was performed using several 3D-molecular descriptors (hydrophobic, steric and electrostatic) which were correlated to the pIC_{50} values. The 3D-QSAR analysis was able to generate two quantitative models with a good correlation between dependent and independent variables as shown in table 2.

Model	Equation	r^2	q^2	*F-test*	*pred_r²*
MLR[a]	pIC_{50} = 1.155 + 13.27(H_2031) - 42.52(E_958)- 16.27(E_2737) + 2.051(E_930)	0.9764	0.9574	89.4679	0.8368
SW[b]	pIC_{50} = 3.493 + 15.382(H_2031) - 4.235(E_1141) + 16.16(S_1275) + 10.06(E_2666) + 0.4279(E_1314) + 157.2(S_1673)	0.9846	0.9782	341.0739	0.8543

Table 2: Selected mathematical models and their statistical validation.

a: MLR means Multivariate Linear Regression; b: SW means Step-Wise regression

In MLR model, hydrophobic (H_2031) and electrostatic (E_930) descriptors contribute favorably to the action while the electrostatic (E_958 and E_2737) descriptors contribute in a negative way (See supplementary information). Finally, it suggests that hydrophobic groups at pyridazine ring increase the biological activity, while electronegative groups are preferable as R-substituent. Based on this, it can explain the excellent activities for the compounds **2-4, 14** and **15**, for example.

SW model suggests that the hydrophobic (H_2031), steric (S_1275 and S_1673) and electrostatic (E_2666 and E_1314) descriptors contribute in a favorable way to the biological activity, while the electrostatic (E_1141) descriptor contributes negatively. This explains the better activity of the compound **21**, which has n = -$(CH_2)_6$-, and NHCOPh, as R-substituent. In addition, bulky groups as R-substituent decrease the biological activity, as observed for the compound 23, with n = -$(CH_2)_6$-, and piperidine, as R-substituent. On the other hand, hydrophobic groups at pyridazine ring and electronegative groups as R-substituent enhance biological activity. Finally, it is noticed that N-substitution of pyridazinone is preferable as R-substituent for PDE4 inhibitory activity, which has already been described in the literature [19].

Other statistical parameters were determined from both models (MLR and SW), such as: component count = 20, degree of freedom = 13 and 16, optimum components = 3 and 6, respectively. The generated models, MLR and SW, have presented satisfactory values in statistical validation step, with $r^2 > 0.6$, $q^2 > 0.6$ and pred_$r^2 > 0.5$, and ¬high Fisher values (F-test).

Finally, it was observed a good agreement between observed and predicted activities in both mathematical models for training (Table 3) and test (Table 4) sets, with their corresponding residual values.

		Predicted pIC_{50}		Residuals	
Code	**Observed pIC_{50}**	**MRL**	**SW**	**MRL**	**SW**
2	6.25	6.93	6.15	0.68	0.1
4	7.69	6.48	7.74	1.21	0.05
5	1.89 [a]	2.86	2.05	0.97	0.16
6	6.6	5.16	6.27	1.44	0.33
7	6.56	5.97	7.16	0.59	0.6
10	1.84 [a]	2.71	1.97	0.87	0.13
11	5.85	4.32	5.49	1.53	0.36
12	5.48	4.32	5.22	1.16	0.26
13	1.76 [a]	2.43	2.01	0.67	0.25
14	6.11	4.91	6.5	1.2	0.39
15	6.22	6.72	6.37	0.5	0.15
16	1.94 [a]	3.33	1.46	1.39	0.48
17	1.93 [a]	2.7	1.95	0.77	0.02
18	1.92 [a]	1.52	1.95	0.4	0.03
19	6.31	5.88	6.12	0.43	0.19
20	7.22	7.63	7.23	0.41	0.01
21	7.52	7.2	6.82	0.32	0.7
22	1.93 [a]	1.24	2.12	0.69	0.19
23	1.2 [a]	1.92	1.45	0.72	0.25
24	7.69	7.81	7.59	0.12	0.1
25	6.74	6.25	6.64	0.49	0.1
26	6.67	6.28	7.02	0.39	0.35
28	6.2	8.48	5.83	2.28	0.37
RP73401	9.0	8.2	9.02	0.8	0.02

Table 3: Observed and predicted inhibitory activities (pIC50), and residual values of the training set generated by MLR and SW mathematical methods.

a: pIC50 value calculated by log (% inhibition)

		Predicted pIC_{50}		Residuals	
Code	**Observed pIC_{50}**	**MRL**	**SW**	**MRL**	**SW**
1	5.69	5.29	5.65	0.4	0.04
3	5.69	6.43	5.62	0.74	0.07
8	6.76	6.89	6.56	0.13	0.2
9	1.41 [a]	2.47	1.61	1.06	0.2
27	6.4	6.04	6.4	0.36	0.0
Rolipram	6.22	6.09	6.2	0.13	0.2

Table 4: Observed and predicted inhibitory activities (pIC50), and residual values of the test set generated by MLR and SW mathematical methods.

a: pIC50 value calculated by log (% inhibition)

Radar plot graphics were generated to analyze the quality of these models, comparing experimental and predicted activities, in training and test sets (Figure 2). It can be observed a slight deviation, indicating highest quality for both models.

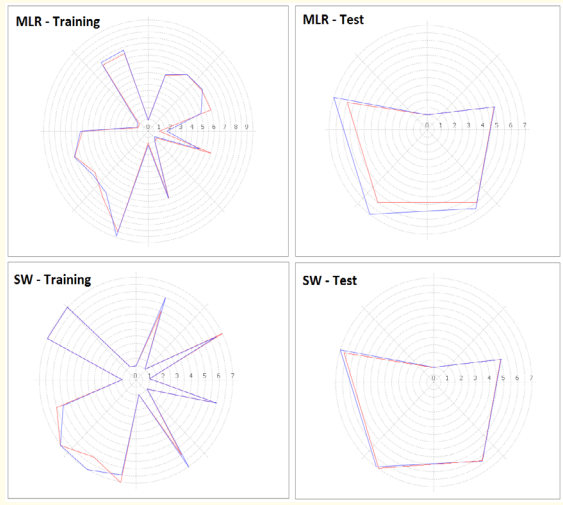

Figure 2: Radar plots showing the alignment of experimental (red) and predicted activity (blue) values for training and test sets, respectively.

3D-QSAR model validation

The generated models can be considered robust, based on values established by Golbraikh., *et al* [25]. The external validation parameter (pred_r^2) is in agreement with Consonni., *et al.* [26], who recommends that pred_r^2 values should be higher than 0.5 and q^2 values lower than r^2 values. In addition, the obtained 3D-QSAR results point that model generated by field analysis were able to provide some important information about features and their relation to the PDE4 inhibitory activity [27].

In figure 3 the cross-validation by LOO method for MRL (A) and SW (B) models is shown and this data indicates great significance in all predictive results.

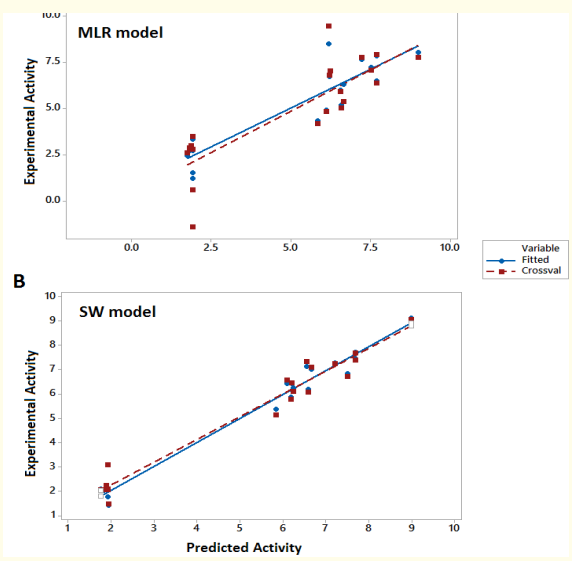

Figure 3: Correlation plot between experimental (blue) and predicted (red) activities using PLS/LOO approach.

Pharmacophore model

Several hypotheses were generated with common features like hydrogen bond donor and/or acceptor and aromatic ring (Figure 4). Pharmacophore model studies revealed that the best compound should contain: two hydrogen bond acceptor groups (HAc 1 and 2) with a distance of 3.546 Å between them; one aromatic ring (AroC4) with a distance of 3.377 Å from HAc1, 6.381 Å from HAc2 and 7.051 Å from a hydrogen bond donor (HDr1); finally, it should contain a central hydrogen bond donor group (HDr1) with a distance of 8.772 Å from HAc1 and 3.87 Å from HAc2 group.

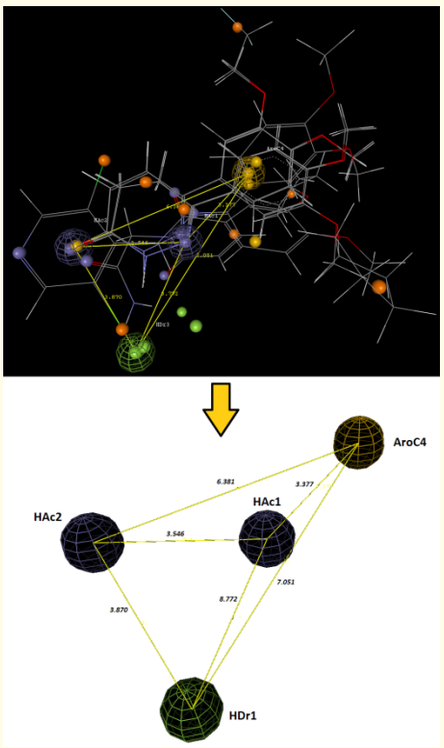

Figure 4: CPharmacophore features for the pyridazin-3-ones PDE4-inhibitors. Green sphere means hydrogen bond donor group; Blue spheres, mean hydrogen bond acceptor group; Yellow sphere, means aromatic ring.

Conclusion

In summary, the 3D-QSAR mathematical models show both great internal and external consistencies. The 3D-QSAR analysis of steric, hydrophobic and electrostatic fields showed that electronegative groups surrounding the pyridazine moiety are required for anti-PDE4 activity, in both models. In addition, the favorable steric field suggests that aromatic bulky groups at pyridazine ring moiety might not be useful for the design of novel structurally related PDE4 inhibitors, in accordance with the model generated by SW method. In addition, both models can be considered robust, reliable and predictive and thus these results could provide a rational basis for the design of more effective analogs. The pharmacophore identification studies revealed which chemical features are important for the inhibitory activity of the PDE4 enzyme. The results reported in this study will advance our understanding of the influence of the distinct chemical structures of inhibitors at the active site (and subsites) and aid the development of new virtual screening protocols to design novel PDE4 inhibitors.

Bibliography

1. Araújo-Júnior JX., *et al*. "Structural optimization of 6-aryl pyridazin-3-ones as novel potent PDE4 inhibitors". *Revista Virtual de Quimica* 7.2 (2015): 744-751.

2. Choudhari P and Bhatia M. "3D QSAR, pharmacophore identification studies on series of 1-(2-ethoxyethyl)-1H-pyrazolo 4,3-dpyrimidines as phosphodiesterase V inhibitors". *Journal of Saudi Chemistry Society* 19.3 (2012): 265-273.

3. Anderson AJ., *et al*. "Enaminones 9. Further studies on the anticonvulsant activity and potential type IV phosphodiesterase inhibitory activity of substituted vinylic benzamides". *Bioorganic and Medicinal Chemistry* 14.4 (2006): 997-1006.

4. Figueiredo LJDO., *et al*. "A chemometric study of phosphodiesterase 5 inhibitors". *Journal of Molecular Graphics and Modelling* 24.4 (2006): 227-232.

5. Kovalishyn V., *et al*. "Predictive QSAR modeling of phosphodiesterase 4 inhibitors". *Journal of Molecular Graphics and Modelling* 32 (2012): 32-38.

6. Srivani P., *et al*. "Molecular modeling studies of pyridopurinone derivatives-Potential phosphodiesterase 5 inhibitors". *Journal of Molecular Graphics and Modelling* 26.1 (2007): 378-390.

7. Cameron RT., *et al*. "Chemical informatics uncovers a new role for moexipril as a novel inhibitor of cAMP phosphodiesterase-4 (PDE4)". *Biochemistry and Pharmacology* 85.9 (2013): 1297-1305.

8. Chakraborti AK., *et al*. "3D-QSAR studies of indole derivatives as phosphodiesterase IV inhibitors". *European Journal of Medicinal Chemistry* 38.11-12 (2003): 975-982.

9. Yang GF., *et al*. "Understanding the structure-activity and structure-selectivity correlation of cyclic guanine derivatives as phosphodiesterase-5 inhibitors by molecular docking, CoMFA and CoMSIA analyses". *Bioorganic and Medicinal Chemistry* 14.5 (2006): 1462-1473.

10. Mitchell CJ., *et al*. "Pyrazolopyridines as potent PDE4B inhibitors: 5-Heterocycle SAR". *Bioorganic Medicinal and Chemistry Letters* 20.19 (2010): 5803-5806.

11. Xiong Y., *et al*. "Characterization of a catalytic ligand bridging metal ions in phosphodiesterases 4 and 5 by molecular dynamics simulations and hybrid quantum mechanical/molecular mechanical calculations". *Biophysic Journal* 91.5 (2006): 1858-1867.

12. Tripuraneni NS and Azam MA. "Pharmacophore modeling, 3D-QSAR, and docking study of pyrozolo1,5-apyridine/4,4-

dimethylpyrazolone analogues as PDE4 selective inhibitors". *Journal of Molecular Modeling* 21.11 (2015): 117-126.

13. Zhmurov PA., *et al*. "Synthesis of PDE IV inhibitors. First asymmetric synthesis of two of GlaxoSmithKline's highly potent Rolipram analogues". *Organic and Biomolecular Chemistry* 11.46 (2013): 8082-8091.

14. Golbraikh A., *et al*. "Data set modelability by QSAR". *Journal of Chemical Information and Modelling* 54.1 (2014): 1-4.

15. Hillebrecht A., *et al*. "Use of 3D QSAR models for database screening: a feasibility study". *Journal of Chemical Information and Modelling* 48.2 (2008): 384-396.

16. Yoo J., *et al*. "3D-QSAR studies on sildenafil analogues, selective phosphodiesterase 5 inhibitors". *Bioorganic and Medicinal Chemistry Letters* 17.15 (2007): 4271-4274.

17. Polanski J., *et al*. "Modeling robust QSAR". *Journal of Chemical Information and Modelling* 46.6 (2006): 2310-2318.

18. El-Kerdawy A., *et al*. "Quantum mechanics-based properties for 3D-QSAR". *Journal of Chemical Information and Modelling* 53.6 (2013): 1486-1502.

19. Krier M., *et al*. "Design of small-sized libraries by combinatorial assembly of linkers and functional groups to a given scaffold: Application to the structure-based optimization of a phosphodiesterase 4 inhibitor". *Journal of Medicinal Chemistry* 48.11 (2005): 3816-3822.

20. Goyal S., *et al*. "Group-based QSAR and molecular dynamics mechanistic analysis revealing the mode of action of novel piperidinone derived protein-protein inhibitors of p53-MDM2". *Journal of Molecular Graphics and Modelling* 51 (2014): 64-72.

21. Sahu NK., *et al*. "QSAR studies of some side chain modified 7-chloro-4-aminoquinolines as antimalarial agents". *Arabian Journal of Chemistry* 7.5 (2014): 701-707.

22. Sharma MC., *et al*. "QSAR studies of some substituted imidazolinones angiotensin II receptor antagonists using Partial Least Squares Regression (PLSR) method based feature selection". *Journal of Saudi Chemistry Society* 17.2 (2013): 219-225.

23. Bhatia MS., *et al*. "Application quantum and physico chemical molecular descriptors utilizing principal components to study mode of anticoagulant activity of pyridyl chromen-2-one derivatives". *Bioorganic and Medicinal Chemistry* 17.4 (2009): 1654-1662.

24. Bhatia MS., *et al*. "Pharmacophore modeling and 3D QSAR studies of aryl amine derivatives as potential lumazine synthase inhibitors". *Arabian Journal of Chemistry* 10.1 (2017): S100-S104.

25. Golbraikh A and Tropsha A. "Beware of q2!". *Journal of Molecular Graphics and Modelling* 20.4 (2002): 269-276.

26. Consonni V., *et al*. "Comments on the Definition of the Q2Parameter for QSAR Validation". *Journal of Chemical Information and Modelling* 49.7 (2009): 1669-1678.

27. Raparti V., *et al*. "Novel 4-(morpholin-4-yl)-N'-(arylidene) benzohydrazides: Synthesis, antimycobacterial activity and QSAR investigations". *European Journal of Medicinal Chemistry* 44.10 (2009): 3954-3960.

Volume 1 Issue 5 November 2017